Stress Optical Behavior in Polystyrene; Residual Stresses and Birefringences in Large, Quenched Samples

C. J. WUST, JR.* and D. C. BOGUE, *Department of Chemical, Metallurgical and Polymer Engineering, University of Tennessee, Knoxville, Tennessee 37996*

Synopsis

In a basic study of the nonequilibrium glassy state of polystyrene, two related areas have been investigated. The first dealt with homogeneous samples and included work on volume aging and the effect of temperature on the stress (and strain) optical coefficients and on the modulus. The second dealt with nonhomogeneous samples and included measurement of the frozen-in birefringence in large, quenched samples and the analysis of this residual birefringence, and also the stress, with residual stress theory. The theory used was that of Aggarwala and Saibel, which is a special case of the more general theory of Lee, Rogers, and Woo.

INTRODUCTION

As extruded or molded parts are shaped and solidified, the surface cools more rapidly than the interior, a cooling history which produces residual ("frozen-in") stresses. The questions of how large such stresses are and what effect they have on the short and long term properties of the material are not easily answered.

There are different kinds of residual stresses and other residual effects, and a clear distinction must be made among them. The present discussion is limited to amorphous materials, and thus crystallization effects will not be considered. Even in the case of amorphous materials, however, it is likely in most fabrication processes that the material is being deformed as it passes through the glass transition temperature (T_g). This deformation produces molecular orientation which will be trapped in the final glassy material. This orientation results in birefringence, and it has been shown that the amount of the latter correlates rather well with the stress at the moment of solidification.[1,2] In general, however, such orientation-induced birefringence does not result in residual stresses. In a homogeneous deformation one removes the stresses at the end of the experiment, resulting in a stress-free but oriented sample. (Orientation induced in this way can, however, produce dramatic changes in the properties[3] and is therefore not a minor consideration.) If the deformation is not homogeneous, nonuniform relaxation of the orientation could result in actual stresses being created, but this is a complication we do not deal with here.

In the present context the term residual stresses refers to those produced by transient thermal gradients, which in practice almost always result in density gradients in the final sample. Physically one can imagine a situation near the

* Present address: Hercules, Incorporated, Research Center, Wilmington, DE 19899.

Journal of Applied Polymer Science, Vol. 28, 1931–1947 (1983)
 CCC 0021-8995/83/061931-17$02.70

beginning of a quench in which the core is still hot but the surface has already cooled below T_g. The core is (largely) able to accommodate the contraction of the cool surface because it is still hot and relaxes quickly. In due time, however, the core also drops below T_g and tries to contract, although it is prevented from doing so and is held under tension by the solidified edges. Since the overall sample is exposed to no external stresses, the final situation is, then, surface layers under compression balanced by center layers under tension. These stresses are the so-called residual stresses.

The qualitative ideas just stated have been put in mathematical form by Lee, Rogers, and Woo (LRW),[4] which follows from the earlier work of Muki and Sternberg.[5] This theory and others related to it have been comprehensively reviewed by Gardon[6] and Wang et al.[7] An instantaneous PVT relationship is assumed in the LRW theory, but in another sense the theory is a viscoelastic one; that is, the nonisotropic residual stresses which are created are allowed to relax with time. Simplifications of the LRW theory are possible, as will be noted later. Inorganic glasses have been treated with considerable sophistication, including time effects, by Gardon[6] and by Gardon and Narayanaswamy.[8] Much less has been done on polymers. Experimental measurements of residual stresses by layer removal methods in thermoplastics have been reported by So and Broutman,[9] Siegmann, Narkis, and Rosenzweig,[10] and in other papers from these groups.[11,12] Struik[13] reports work on the compressive behavior of the surface. Work on thermosets has been done by Shen.[14] The most extensive work is that of the injection molding group at Cornell University.[15,16]

The experimental measurement of residual stresses is not easy. The technique involves removing layers of the material and measuring the small bending that occurs as the stresses are thus relieved. Much easier to measure but more difficult to interpret are the residual birefringences. When prior deformation has occurred, the birefringence reflects both orientation and volume (residual stress) effects. Even in the absence of prior flow, the analysis is complicated by the fact that the final birefringence must depend on some weighted thermal history of the point in question and not just on its final state. Nonetheless, the ease with which birefringence is measured and the ability to use this technique on samples of complicated shape led us to attempt a quantitative interpretation.

In preparation for doing such an interpretation we undertook certain basic, preliminary studies on small (presumably homogeneous) samples. These studies dealt with volume–temperature–time relationships in both the rubbery and the glassy states and the treatment of these data with a first-order rate expression with stress (or strain) optical behavior, and with stress–strain (i.e., modulus) behavior. Since this work stands on its own, as basic studies in these areas, we present the data here for future reference, even though, finally, not all of them were used in the analysis of the residual birefringences.

EXPERIMENTAL DETAILS AND PRESENTATION OF RESULTS

The material used throughout was a commercial polystyrene, Shell TC 3-30, which we have used in a number of previous studies and have characterized in various ways.[3,17] Its molecular weight parameters are $M_w = 2.83 \times 10^5$ and $M_w/M_n = 4.6$.

Homogeneous Samples

Experimental. The term "homogeneous samples" refers to samples which are small enough to be substantially free of temperature gradients across them as they are cooled. In previous work[18] we decided that fiber samples of the order of 400 μm in diameter (or smaller) were almost homogeneous up to cooling rates of about 1°C/s. Samples quenched in water, however, certainly experience faster cooling rates than that, although at what level gradients must be termed "significant" is difficult to judge. In the volume aging studies we found it necessary to use fiber samples of about half that size (about 200 μm) to obtain reproducible results. Such samples were heated to 120°C in air oven, held there for at least 30 min, and then quenched in various ways: by cooling them in the temperature-controlled air oven[3,18] (at cooling rates up to 1°C/s) or by removing them and quenching them in ice water. The samples so obtained were placed in a density gradient column (containing a mixture of ethylene glycol and water), and the densities were observed over a period of time.

Separate from these volume aging studies, we needed systematic data on the optical behavior and also on the extensional modulus, as a function of temperature, to be used in the analysis of residual stresses. These studies were mostly carried out on filmlike samples 2 mm thick and 10 mm wide, of varying lengths. Because here the experiments were carried out under isothermal conditions, ranging from below T_g (25°C) to above it (105°C), it was not necessary to be concerned about temperature gradients across them, and thus thicker samples could be used. In the tensile birefringence measurements the length of the samples was 50 mm. In the tensile modulus measurements the length was varied between 12.5 and 175 mm. These were held with pneumatic grips in an Instron tensile tester and pulled at rates of 0.4%/min and 0.8%/min, with most of the runs (and all of the data reported here) being at the former rate. The use of various gauge lengths (L) was suggested by the work of Patel and Bogue,[19] who noted significant instrument compliance effects. Following their suggestion the reciprocal of the apparent modulus was plotted against $1/L$ and extrapolated to infinite L to obtain the true modulus. Such correlations were not necessary above about 102°C because of the large strains involved. In addition, some other samples, measuring ¼ in. × ¼ in. × 1 in., were subjected to compressive testing. The compression apparatus was designed to permit measurement of stress and of the birefringence but was not rigid enough for the measurement of strain (see Ref. 20 for details). It was thus assumed in subsequent calculations that the unknown compression modulus was the same as the measured tensile modulus.

The samples were subjected to a given elongational or compressional force at some constant temperature, and the birefringence and the stress were measured immediately, meaning within 2 or 3 s. The birefringence (Δn) was measured with a Babinet compensator, for low levels, or with a 10- or 30-order Leitz–Wetzlar compensator, for higher levels. The sample was viewed through glass windows surrounding the air oven with a 100× optical microscopic mounted on a micrometer slide. (Essentially the same optical setup was later used in the measurement of the birefringence profiles in the large quenched slabs.) In the filmlike samples Δn was also observed over time and at various stress levels.

Results. The volume aging data on samples quenched in various ways are

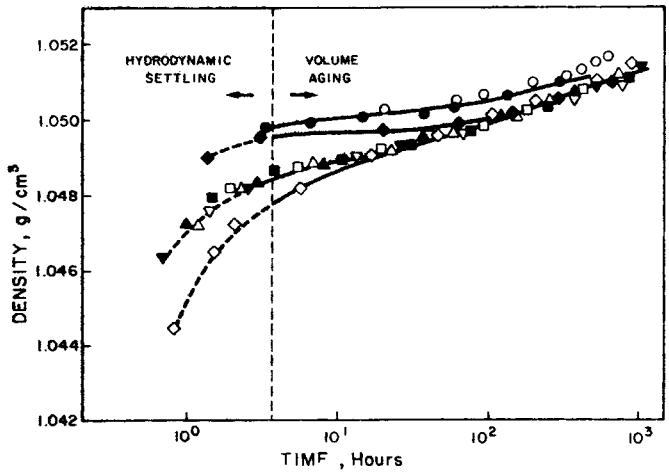

Fig. 1. Volume aging of glassy samples after cooling from 120°C at various rates. Quench rates (°C/s): (◇) ≈ 40; (●) 0.0038; (○) 0.0055; (◆) 0.016; (□) 0.19; (■) 0.37; (△) 0.50; (▲) 0.68; (▽) 1.05; (▼) 1.13.

presented in Figure 1. Because of hydrodynamic drag, the samples do not immediately reach their equilibrium positions in the density gradient column. Observations made with pre-aged samples suggested that time periods up to 3–4 h were necessary for the settling due to hydrodynamic drag to occur; this is a conservative estimate and thus it is felt that the data at times greater than 4 h

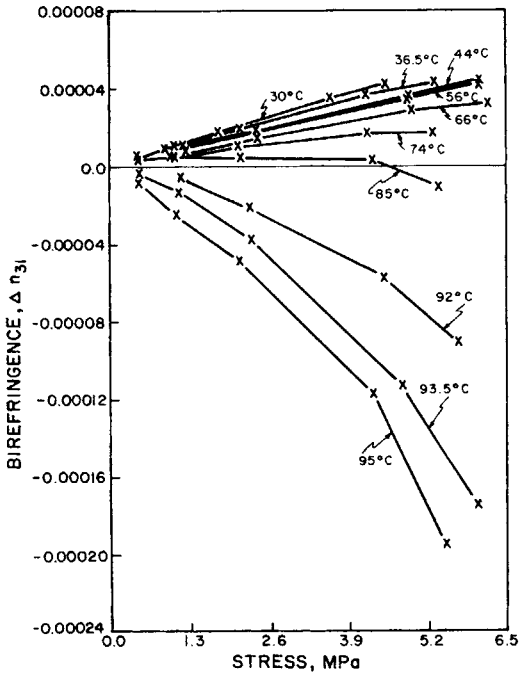

Fig. 2. Short-time birefringence as a function of stress and temperature.

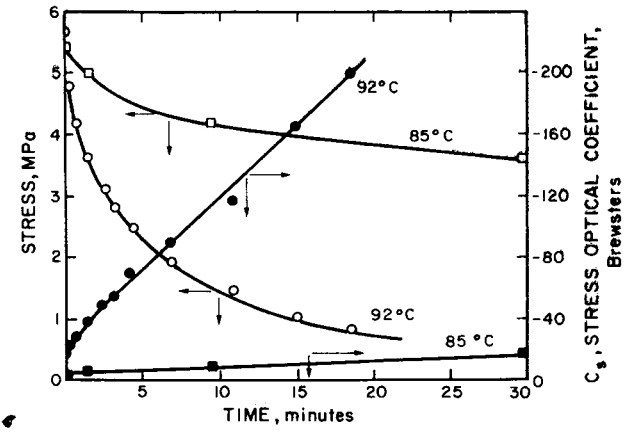

Fig. 3. Variation of stress and stress optical coefficient with time, at temperatures near T_g.

(to the right of the dotted line) are reliable in judging volume aging. Although the so-called "free volume" is probably changing significantly, the total volume (as shown on the ordinate) does not. However, a number of different runs were made, and there is good internal consistency. We estimate the error to be no more than 0.0002 g/cm^3, or, in other words, the uncertainty is comparable to the size of the symbols shown in Figure 1. As expected, rapidly quenched samples have smaller (more rubbery-like) densities than slowly quenched ones and age faster. Efforts at fitting such data with a first-order rate equation will be noted briefly in the next section.

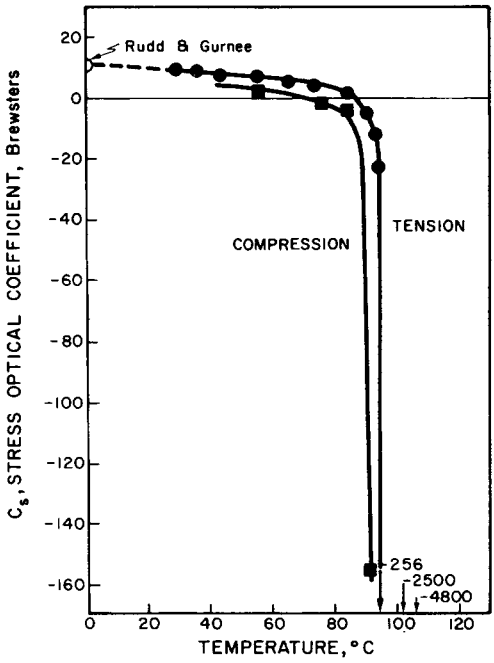

Fig. 4. The stress optical coefficient as a function of temperature.

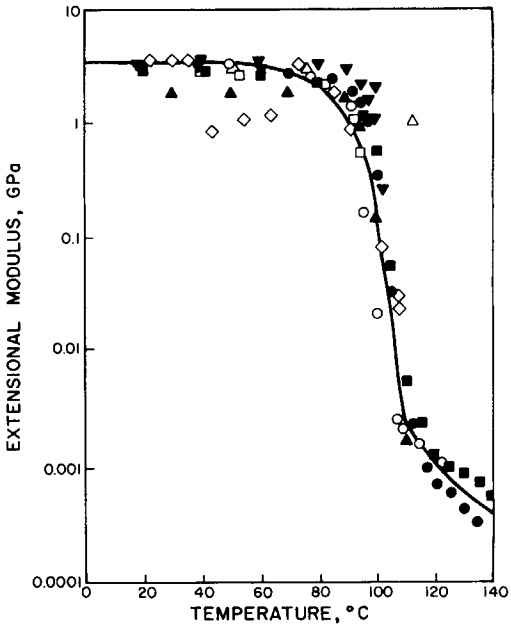

Fig. 5. Extensional modulus as a function of temperature. Reference numbers: (○) 25; (□) 26; (△) 27; (▼) 28; (▲) 29; (■) 30; (●) 31; (◇) present work.

The data on optical behavior and modulus as a function of temperature are presented in Figures 2–6. We are dealing here with samples that have been pulled at various temperatures, with the temperature being held constant during each set of measurements. The stress and the birefringence are monitored as a function of time. The short-time (about 2–3 s) birefringence as a function of stress level is shown in Figure 2 and the variations of stress and stress optical coefficient [see eq. (1) below] as a function of time are shown in Figure 3. Additional data, at lower temperatures, are available in the dissertation.[20] The short-time, low-stress birefringences are reasonably linear in stress, and these data are plotted as stress optical coefficients in Figure 4. The stress optical coefficient C_s is defined by the relation

$$\Delta n = C_s \Delta \sigma \tag{1}$$

where $\Delta\sigma$ is the difference in the principal stresses, the other symbols having been previously defined. The stress optical coefficient is reported in units of Brewsters, where 1 Br = 10^{-13} cm^2/dyn.

The stress optical behavior is obviously not simple. The coefficient C_s is in good agreement with the literature in the extremes of a very glassy state or a very rubbery state, with literature values being about +10 Br for the former (see, for example, Ref. 21) and typically about −5000 Br for the latter (see Refs. 1, 2, and 20 for a review of the references). The only data known to us at intermediate temperatures are those of Tsvetkov and Krym.[22] In their data the crossover from positive to negative C_s occurs at about 50°C and the precipitious drop (to −4100 Br) occurs at almost exactly 100°C. Their data are thus qualitatively but not quantitatively in agreement with ours, the sudden drop in our coefficient

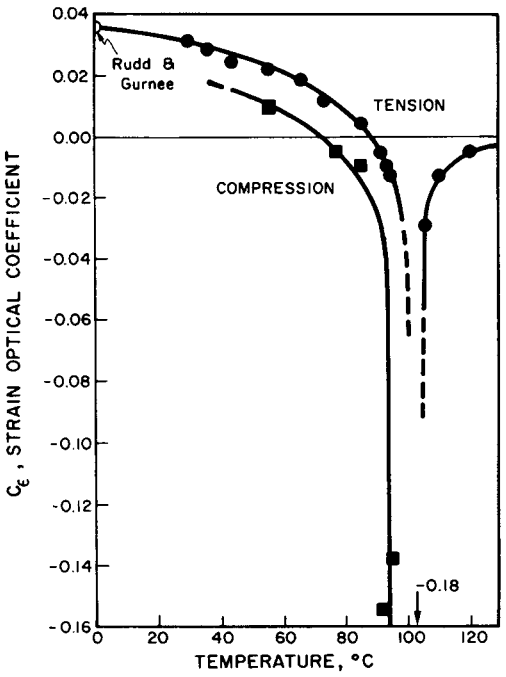

Fig. 6. The strain optical coefficient as a function of temperature: $C_\epsilon = 0.016095 \cdot \ln[(100 - T)/10] - 0.00183$.

occurring at about 92°C. These differences are probably due to time (and possibly stress level) effects; there are few details on these variables in their work. Clearly there are two different mechanisms in the two extremes of temperature. The rubbery (or negative) mechanism involves the aligning of the phenyl groups which become increasingly parallel with each other (and are attached to the backbone at a fixed angle) as the chains become increasingly aligned[21,23,24]; this mechanism is thus associated with molecular orientation. The glassy (or positive) mechanism, which must take place quite rapidly, is somehow associated with the deformation of the now-rigid backbone and the benzene rings which are attached to it.[23] Little or nothing is known about additive effects—i.e., the glassy behavior of previously oriented samples. We performed a few experiments of this kind,[20] and the subsequent glassy experience seemed always to add a positive birefringence, although time effects complicate any interpretation. The time-dependent data of Figure 3 rather clearly suggest that the phenyl group orientation (associated with the negative birefringence) takes place over some period of time at temperatures in the range of 85–92°C and does not correspond simply with the stress. This is in contrast to the behavior at high temperatures (well into the rubbery state), where stress and birefringence are proportional (see Refs. 1 and 2). We note a small but consistent effect of the sign of the stress (tension vs. compression), but do not suggest a specific mechanism, except possibly the differing effect of the deformation on volume (a Poisson's ratio effect) in the two cases. Obviously the details of the birefringence behavior in the transition region are complicated and will require further study. For later parts

of the present work, we used the short-time, low-stress coefficients as shown in Figure 4.

The corresponding data for the short-time, low-stress extensional modulus, as a function of temperature, are shown in Figure 5 and compared with a variety of literature values. Many of these data come from dynamic measurements and the value shown is that for G' at high frequency except where noted; where shear, rather than extensional, modulus was measured, the values at the lower temperatures (below 102°C) have been multiplied by 2.67, which presumes a Poisson's ratio of about 0.33, whereas those at the higher temperatures have been multiplied by 3.0. Schmieder and Wolf[25] and Nielsen, Wall, and Richmond[26] measured the dynamic shear modulus. Wall, Sauer, and Woodward[27] used a resonance technique. Newman and Cox[28] used both a torsional pendulum and a vibrating reed technique, while Tobolsky and Takahashi[29] and Takahashi et al.[30] reported torsional moduli at 10 s. Schwarzl[31] measured torsional creep compliance after 16 s. Considering the variety of techniques used the data are in surprisingly good agreement. Since our own data are somewhat low at the lower temperatures, it seemed better to use the average line, as shown, as the best estimate of the modulus in the subsequent calculations.

Finally, for the purpose of analyzing the residual birefringence data it was convenient to calculate strain coefficient C_ϵ defined by

$$\Delta n = C_\epsilon \Delta\epsilon \tag{2}$$

where $\Delta\epsilon$ is the difference of principal values of the linear strain. The strain optical coefficient was, in fact, obtained by multiplying the values shown in the two curves in Figure 4 by the smoothed modulus data (Fig. 5). The same modulus was used in both tension and compression, as previously noted. The results for the strain optical coefficient are shown in Figure 6. For later use a least squares fit of the tension data to an empirical equation was made, the equation being shown on Figure 6. The use of the tension curve, rather than the compression curve, was an arbitrary decision, based mostly on the fact that we had considerably more data in the former case.

Nonhomogeneous Samples

Experimental. For the work on residual birefringences, slablike samples (1/4 in. × 1 in. × 2 in.) were prepared by melting the material in a heated mold and cooling to room temperature over 6–8 h. Considerable care was needed to achieve bubble-free, stress-free samples.[20] Birefringence transverses of the starting samples showed no measureable values of Δn. These samples were then heated to 120°C in the air oven and cooled in four ways: (1) by blowing room air over them in the air oven (air quench), (2) by plunging them into a beaker containing water and ice at 0°C (ice water quench), (3) by plunging them into ethylene glycol containing dry ice at temperatures between −38°C and −50°C (glycol quench), and (4) by plunging them into a Dewar flask containing liquid nitrogen at −196°C (nitrogen quench). To determine the time-temperature histories of these quenched slabs, small thermocouples (0.01 in. in diameter) were inserted at the center line (the center line of the 1/4 in. dimension) and at a midway point between the centerline and the surface (that is, at 1/16 in. from these planes). By monitoring these temperatures as a function of time and using standard

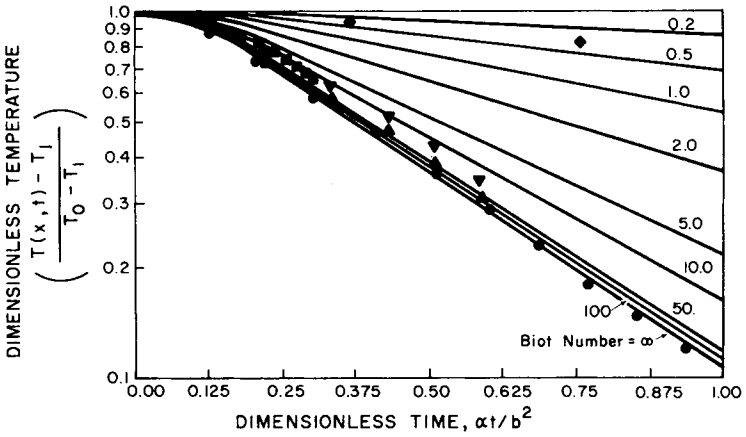

Fig. 7. Centerline temperature of quenched slabs fit to transient heat transfer theory. Quench: (●) ice water (0°C); (■) liquid nitrogen (−195.8°C); (◆) forced air (25°C); (▲) dry ice/glycol (−38°C); (▼) dry ice/glycol (−50°C).

transient heat transfer theory (see, for example, McAdams[32]), it was possible to obtain good theoretical predictions. In doing that we set the surface heat transfer coefficient (h) at 10, infinity, and 330 J/(s·m^2·°C) [1.8, infinity, and 58 BTU/(h·ft^2·°F)], for the air quench, the ice water quench, and the nitrogen quench, respectively. The final fit of the center line temperature to theory is shown in Figure 7. The finite value for h for the nitrogen quench, as compared with a nearly infinite value for the ice water quench, is undoubtedly due to the presence of film boiling in the former case. Thus the transient heat transfer equations which lie behind the curves in Figure 7 could be used with confidence to calculate the time–temperature histories needed in the subsequent analysis.

Samples so quenched were sliced in various ways (as shown in Fig. 8) and polished. The cutting was done on a Gillings–Hamco thin-sectioning machine and the surfaces polished with decreasingly smaller abrasive materials, ending

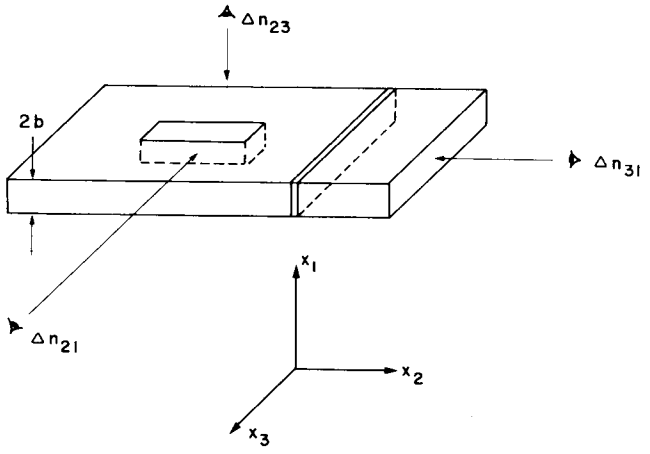

Fig. 8. Schematic diagram of slab used in residual birefringence measurements and analysis.

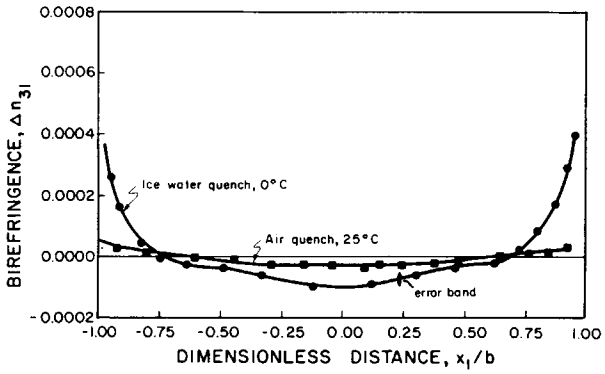

Fig. 9. Measured birefringence profiles for ice water and air quenched samples.

with a 9.5 μm aluminum oxide powder on a polishing wheel. For control, as-molded samples were also sliced and polished and showed no detectable Δn. Apart from the matters of cutting and polishing were the questions of sample symmetry and sample thickness. Samples were cut as shown in Figure 8 and the three Δn's measured. The birefringences Δn_{31} and Δn_{21} were identical, and Δn_{23} was zero within experimental error. Furthermore, samples of various thicknesses, varying from 0.8 mm to 6.8 mm, were studied. This was done at the suggestion of Gardon,[33] who noted that the slicing itself relieves stresses at the cut surface. There was no detectable effect of the sample thickness and thereafter a sample thickness of 4.3 mm was used. Average curves for both the air quench and water quench are shown in Figure 9.

Results. Several interesting qualitative observations were made during the quenches. The nitrogen-quenched samples shattered almost immediately due to excessive thermal stresses. The glycol-quenched samples fractured as they warmed back to room temperature, and the fracture occurring in an interesting way. Cracks formed internally but did not progress to the surface, apparently due to the highly compressive layer there. Because of the fractured samples in these two cases, only the ice water quench and the air quench could be studied further.

Average curves for these two quenches are shown in Figure 9. The error band reflects the scatter in a large number of runs, including those made with various sample thicknesses and replicate runs (five or more) at constant thickness. The profiles are qualitatively as expected. There is a marked gradient across the cross section, the more so when a large temperature gradient has been imposed (the ice water quench); furthermore, there is a change of sign as one moves from the surface to the center, consistent with the physical picture developed earlier of a differing contraction history of these two positions. But further understanding, particularly regarding the sign of the birefringence, requires a theoretical analysis.

ANALYSIS OF RESULTS

Rate of Volume Change in Homogeneous Samples

There is a considerable literature using the concept of a "free volume" as a state variable to characterize the rheological response of both the rubbery and glassy

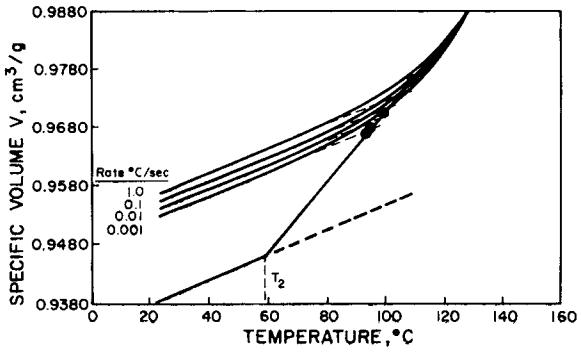

Fig. 10. Predicted volume-temperature curves at various cooling rates; compared with data for apparent T_g's at various rates (°C/s): (●) exptl T_g's at 1.0, 0.1, 0.01, and 0.001 (Wust, Ref. 20).

states. This has led to several rate equations for volume, as summarized up to 1967 by Goldbach and Rehage[34] and Kovacs.[35] Recent reviews are those of Kovacs et al.,[36] Struik,[37] and Tant and Wilkes.[38] We here use a first-order rate equation due to Rusch,[39] which seemed to us to incorporate the essential physical ideas in explicit form. Rusch's equation is

$$\frac{dV}{dt} = -\frac{(V - V_e)}{\tau_R a_{T,V}} \tag{3}$$

where V is the specific volume (cm³/g) at any time t, V_e is the equilibrium volume at the temperature existing then, τ_R is a time constant at some reference temperature, and $a_{T,V}$ is a shift factor which depends on both temperature and the instantaneous free volume. The essential physical data can be understood by considering the curves of Figure 10. It is supposed that there is an underlying equilibrium volume there, although this may never in fact be achieved in the glassy state. For mathematical reasons it is convenient to use one thermal expansion coefficient in the rubbery state and another one in the glassy state and to change from one to the other at a specific temperature. We label that temperature T_2 (= 59°C), to use Rusch's notation and value. This implies a second-order transition at T_2, but the sharp break there is not essential to the rate argument and a "rounding off" of the equilibrium curves at T_2 does not affect the physical ideas involved. There is, however, an implicit assumption that an equilibrium state of some sort does exist. For convenience we model this equilibrium state with linearized coefficients of expansion as follows

$$V_e = V_0\,\alpha_L(T_0 - T) \qquad \text{(above } T_2\text{)} \tag{4}$$

$$V_e = V_0 - \alpha_L(T_0 - T_2) - \alpha_G(T_2 - T) \qquad \text{(below } T_2\text{)} \tag{5}$$

where V_0 = 0.9824 cm³/g (at 120°C), α_L = 0.0060 cm³/(g·°C), α_G = 0.0021 cm³/(g·°C), and T_0 = 120°C (an arbitrary starting temperature). These values for the physical constants are estimated from the work of Richardson and Savill.[40] The "free volume" is defined as the difference between the actual volume existing at the moment of consideration and the underlying *glassy* equilibrium volume, extrapolated above T_2 if the instantaneous temperature happens to be there. Thus, at high temperatures there is the concept of an equilibrium free volume, but at temperatures below T_2 any free volume is necessarily nonequilibrium.

Finally, following Rusch, the shift factor equation is given by

$$\log a_{T,V} = \frac{-C_1(T_e - T_R)}{C_2 + T_e - T_r} \tag{6}$$

where

$$T_e = T + \frac{V - V_e}{\alpha_L - \alpha_G} \qquad \text{(above } T_2\text{)} \tag{7}$$

or

$$T_e = T_2 + \frac{V - V_e}{\alpha_L - \alpha_G} \qquad \text{(below } T_2\text{)} \tag{8}$$

The form of eq. (6) is, of course, that of the familiar Williams, Landel, and Ferry (WLF) equation,[41] except for the appearance of the symbol T_e (the "effective" temperature) in lieu of the actual temperature T. The quantity T_e is the temperature the material would hypothetically have if its actual (possibly nonequilibrium) free volume were to be calculated by equilibrium equations. Under equilibrium conditions T_e is the actual temperature T, but under nonequilibrium conditions T_e is substantially larger than the T because of the frozen-in free volume. Following the prior work,[39] the constants used in these equations were $C_1 = 12.4$, $C_2 = 41°C$, and $T_R = 100°C$. Using τ_R as an adjustable constant, set at 5000 s, predictions of volume vs. time were run off by computer at various linear cooling rates R(°C/s) as shown in Figure 10. "Breakaway" points—i.e., the points of departure from the equilibrium rubbery line—are marked with short dotted lines and can be thought of as apparent glass transition temperatures [T_g(app)]. In prior work[3] we measured T_g(app) by an indirect method—by noting the buildup of force in a clamped sample—not by direct measurement of the volume, which is difficult if not impossible to do at the high cooling rates involved. The data from this experiment [T_g(app) vs. R], which we consider reliable up to a cooling rate of about 1°C/s, provide the experimental points shown in Figure 10. The first-order rate theory, with τ_R as an adjustable constant, does, then, give a reasonable prediction for the experimental values of T_g(app). We also attempted to use eq. 3 to predict the subsequent volume aging of the quenched samples (i.e., the data of Fig. 1), but we were not successful in doing that without arbitrarily introducing a new (and much larger) time constant τ_R. Further work on a generalized rate equation, which deals with the difficulty just noted and also with combining the volume and the nonisotropic deformation terms into one equation, is being carried out by Snow.[42]

For the subsequent work it should be noted that an important property of eq. (3) is that the effective temperature T_e is essentially set at the "breakaway" point [i.e., at T_g(app)]. The nonequilibrium free volume hardly changes thereafter, making T_e essentially constant, even as the actual temperature drops to ambient conditions.

Residual Stresses and Birefringences in Large, Quenched Samples

A major emphasis of the present work was on the analysis of residual stresses and birefringences, and the measurement of the latter, in large, rapidly quenched samples. The quenching and slicing of the samples, shown in Figure 8, is de-

scribed in the experimental section. Although we measured residual birefringences, the theory is cast in terms of residual stresses, and we therefore present the basic equations in that form. The most general treatment is that of Lee, Rogers, and Woo (LRW),[4] who imagine a slab similar to that shown in Figure 8 but of infinite extent in the 2 and 3 directions. One must imagine a solidification of the extremities, however, because there must be a mechanism for averaging out the stresses there (and in fact elsewhere along the 2 and 3 directions). That is,

$$\int_0^b \sigma(x_1, t) = 0 \tag{9}$$

where $\sigma = \sigma_{22} = \sigma_{33}$. With various assumptions, this "squeezing stress" (σ) is given by

$$\sigma(x_1, \xi) = \int_0^{\xi} 2G(\xi - \xi') \frac{\partial}{\partial \xi'} [\epsilon_2(\xi') - \epsilon_1(x_1, \xi')] d\xi' \tag{10}$$

where ξ is a reduced time, expressed in terms of the real time and a shift factor, $G(t - t')$ is a relaxation modulus, and $\epsilon_2 = \epsilon_{22}(t) = \epsilon_{33}(t)$ and $\epsilon_1 = \epsilon_{11}(x_1, t)$ are linear strains. The trace of stress σ_{kk} is presumed to be instantaneously rated to the volume change (ϵ_{kk}) and the temperature change (i.e., an instantaneous PVT relation is assumed), cast in terms of a compressibility factor and a thermal coefficient of expansion. As implied by Wang et al.[7] and shown in some detail by Wust,[20] this general theory can be reduced to the simpler theory of Aggarwala and Saibel[43] by imagining rheological behavior in which G is zero above some critical temperature (T_g) and a large constant below (i.e., the material either has no memory at all or complete memory). After a number of steps eq. (10) reduces to

$$\sigma(x_1, t) = \int_{\bar{t}(z)}^{t} 6\beta \left\{ \frac{1}{b - \bar{z}(t)} \int_{\bar{z}(t)}^{b} \frac{\partial}{\partial t'} [\alpha T(x_1', t')] dx_1' - \frac{\partial}{\partial t'} [\alpha T(x_1, t')] \right\} dt' \tag{11}$$

where $\bar{t}(z)$ is the time at which a particular position z passes through T_g, $\bar{z}(t)$ is the position of the solidification line at any time t, α is the thermal coefficient of expansion, and β is given by

$$6\beta = E/(1 - \nu)$$

where E and ν are the instantaneous Young's modulus and Poisson's ratio, respectively. Equation (11) is the theory of Aggarwala and Saibel[43] and was used in the analysis here.

For the prediction of stress one needs to assume a value of 6β. Taking it as constant (at $6\beta = 4.9$ GPa), one obtains stresses in order-of-magnitude agreement with the stress data of the Cornell group[7,16] obtained on water-quenched samples. The theory of eq. (11) does, however, call for a time-dependent value of the modulus, averaged over the history of the sample as shown, and not simply for a constant. Other work of this type, including a treatment using a constant modulus and one using an approximation of the full LRW theory, has been done by the Cornell group.[7]

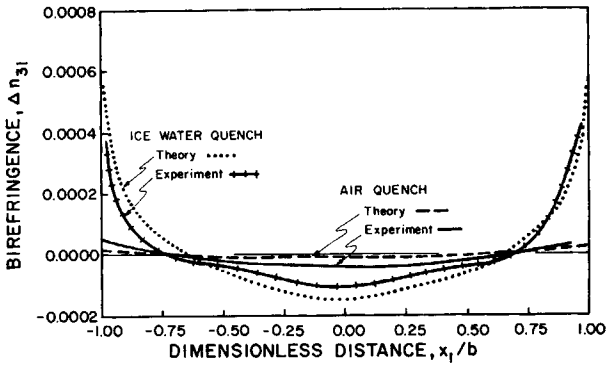

Fig. 11. Prediction of birefringence profiles assuming a constant strain optical coefficient.

For our work we need to replace the modulus G (or 6β) with a properly time- and temperature-dependent (or perhaps constant) strain optical coefficient. We tried several assumptions in an effort to fit the observed Δn profiles of Figure 9. The simplest assumption, of course, is to take the coefficient as a constant. Since

$$\Delta n = C_s\sigma = C_\epsilon\sigma/E \qquad \text{and} \qquad 6\beta = E/(1-\nu)$$

one replaces 6β in eq. (11) by $C_\epsilon/(1-\nu)$ where C_ϵ and ν are taken as constants, with values of -0.012 and 0.33, respectively. The value -0.012 corresponds to 94°C, using the tension curve of Figure 6. The predicted profiles are shown in Figure 11 and are in reasonable agreement with experiment. To justify the assumption of constant C_ϵ, however, one must imagine that all of the "action" takes place at about 94°C, which is not consistent with the physical picture that a great deal of the residual stress (and one presumes a great deal of the residual birefringence) is put in during the subsequent cooling down to room temperature. It is conceivable that birefringence might have to be treated quite differently, such that the analysis for it is simply "discontinued" as a given point passes through T_g. If so, a major restructuring of the theory, or of the connection between birefringence and stress, will be needed.

In order, however, to stay within the framework of existing theory, we tried several other assumptions, including one involving a temperature-dependent (but not time -dependent) function of C_ϵ (using the equation shown in Fig. 6); this assumption gave profiles of reasonable shape and magnitude but reversed in sign, i.e., negative Δn at the surface and positive Δn at the center. This comes about physically because of the sign change of C_ϵ (see Fig. 6) and the importance of the positive C_ϵ part of the temperature history in the cooling from 94°C to the final temperature. To find a reasonable explanation for the observed data we returned to eq. 3, the rate equation for the volume, which involves the physical idea of an "effective temperature" (T_e) as the characterizing parameter for the nonequilibrium glass. As noted in the discussion following eq. (3), T_e remains almost constant after the volume departs from the rubbery volume line [i.e., below T_g(app)]. Using values for T_e and T_g(app) calculated from eq. (3) and for typical cooling rates, we calculated the birefringence profiles shown in Figure 12. The typical cooling rates used were 0.1°C/s and 1.0°C/s for the air quench and the ice water quench, respectively. Of course, the surface cools very rapidly, but

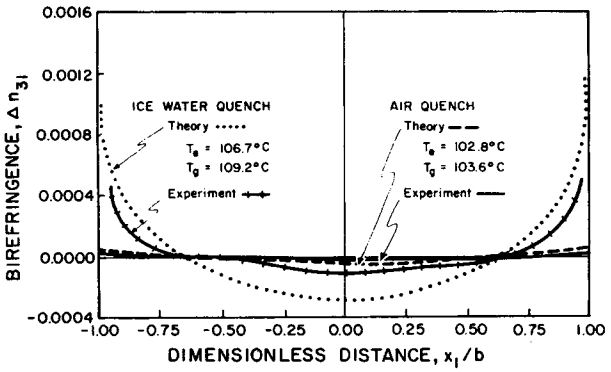

Fig. 12. Prediction of birefringence profiles assuming a strain optical coefficient dependent on an effective temperature.

the interior portions cool at a fairly constant rate as the heat transfer becomes controlled by the thermal conductivity of the solid. The T_e and T_g(app) values actually used are shown on Figure 12. The fits are satisfactory, although perhaps not as good as in Figure 11; we view the better fit in Figure 11 as probably fortuitous. In any case the actual values for C_ϵ used in the two figures are not greatly different because the effective temperature T_e (and thus C_ϵ) is taken as constant shortly after the material passes into the glassy state. Given the complexity of the birefringence–temperature–time relationships, as shown in Figures 2–4, we do not view our analysis as definitive, but the degree of fit in Figures 11 and 12 suggests tht it is plausible. We are continuing our studies, with emphasis on other materials and on different thermal histories.

Finally, it is of interest to look at the theoretical predictions for the transient dimensionless stress (actually strain, but imaginable as stress if the modulus is taken as constant), as shown in Figure 13. These transient predictions [from eq. (11)] show the complex development leading to the final stress profile (that marked 365.3 s). One notes that the surface is initially under tension, at times when only the surface layers are solidified, with the appearance of the expected signs (center under tension, surface under compression) occurring only after the center line has solidified. The discontinuity at very short times is a computer difficulty because of the extremely rapidly changing temperature gradients near the surface. Transient profiles similar to Figure 13 have been presented by Narayanaswamy and Gardon.[8]

CONCLUSIONS

1. A simple first-order rate equation for the volume, involving a shift factor dependent on free volume as well as temperature, is of the right form for dealing with the rapid cooling of a rubbery material into the transition regime. Such an equation can be used to correlate T_g data [of the form of T_g(app) vs. cooling rate] with one adjustable time constant. Efforts to use the same equation to deal with the long-term aging of the quenched samples were not successful without making an arbitrary adjustment of the time constant. We have made progress in reconciling these diverse experiments into a single rate expression in more recent work (Snow[42]).

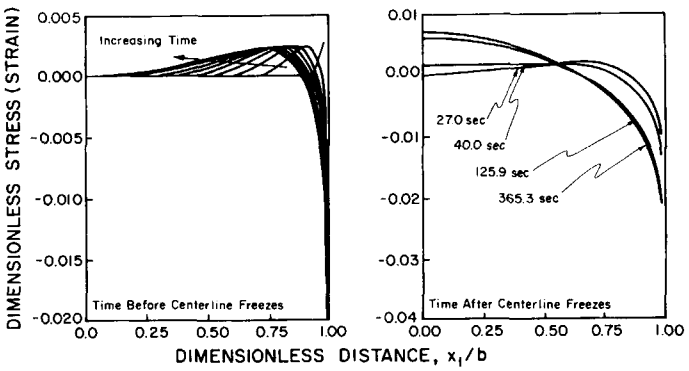

Fig. 13. Theoretical prediction of transient dimensionless stress (or strain) profiles for an ice water quench. Time increments (s): 0.20, 2.56, 5.12, 7.69, 10.25, 12.82, 15.37, 17.93, 20.50.

2. Basic studies of birefringence as a function of temperature and time showed complex relationships, especially in the transition region between the rubbery and glassy states. Nearly constant stress (or strain) optical coefficients appear in the limits of very glassy or very rubbery behavior, but there are not simple proportionalities in the intermediate regime. Notably, the negative birefringence which is characteristic of polystyrene in the rubbery regime develops only slowly with time, at temperatures just below T_g, although the stress develops quickly there. All of these experiments started with stress-free samples at a given temperature; the subsequent work on residual birefringence suggests that the short-term response of rapidly quenched samples is probably much more complicated.

3. Residual birefringences (as an indicator of residual stresses) appear in large, rapidly quenched samples, as a result of the different thermal experience of the surface as compared with the center. Such residual birefringences can be predicted using the theory due to Aggarwala and Saibel (a special case of the more general theory of Lee, Rogers, and Woo), by invoking the plausible (but certainly not proven) concept of an "effective temperature" as the characterizing variable for the nonequilibrium glassy state.

The authors acknowledge with thanks the support of the National Science Foundation, which provided the basic research funds under Grant No. CPE 7925104. The first author also acknowledges the generous help of the Plastics Institute of America, which provided financial support thrcugh the William B. Bradbury Fellowship. Finally, the most useful comments and reports of Dr. Robert Gardon and Dr. A. I. Isayev are gratefully acknowledged.

References

1. K. Oda, J. L. White, and E. S. Clark, *Polym. Eng. Sci.*, **18**, 53 (1978).
2. T. Matsumoto and D. C. Bogue, *J. Polym. Sci.*, **15**, 1663 (1977).
3. D. A. Carey, C. J. Wust, Jr., and D. C. Bogue, *J. Appl. Polym. Sci.*, **25**, 575 (1980).
4. E. H. Lee, T. G. Rogers, and T. C. Woo, *J. Am. Cer. Soc.*, **48**, 480 (1965).
5. R. Muki and E. Sternberg, *J. Appl. Mech.*, **28**, 193 (1961).
6. Robert Gardon, in *Glass: Science and Technology*, D. R. Uhlmann and N. J. Kreidl, Eds., Academic, New York, 1980, Vol. 5.
7. K. K. Wang, S. F. Shen, C. Cohen, C. A. Hieber, A. I. Isayev, and T. Akiyama, Progress Report No. 7, Injection Molding Project, Cornell University, Ithaca, 1980.

8. O. S. Narayanaswamy and R. Gardon, *J. Am. Cer. Soc.*, **52,** 554 (1969); R. Gardon and O. S. Narayanaswamy, *ibid.*, **53,** 380 (1970).
9. P. So and L. J. Broutman, *Polym. Eng. Sci.*, **16,** 785 (1976).
10. A. Siegmann, M. Narkis, and N. Rosenzweig, *Polym. Eng. Sci.*, **19,** 223 (1979).
11. B. S. Thakkar and L. J. Broutman, *Polym. Eng. Sci.*, **20,** 1214 (1980).
12. A. Siegmann, A. Buchman, and S. Kenig, *Polym. Eng. Sci.*, **22,** 40 (1982).
13. L. C. E. Struik, *Polym. Eng. Sci.*, **18,** 799 (1980).
14. Y. C. Shen, M. S. thesis, University of Tennessee, Knoxville, 1981.
15. A. I. Isayev, C. A. Hieber, and D. L. Crouthmel, *SPE ANTEC Tech. Papers*, **27,** 110 (1981).
16. D. L. Crouthmel, A. I. Isayev, and K. K. Wang, *SPE ANTEC Tech. Papers*, **28,** 295 (1982).
17. R. Racin and D. C. Bogue, *J. Rheol.*, **23,** 263 (1979).
18. T. Matsumoto and D. C. Bogue, *Trans. Soc. Rheol.*, **21,** 453 (1977).
19. P. D. Patel and D. C. Bogue, *Polym. Eng. Sci.*, **21,** 449 (1981).
20. C. J. Wust, Jr., Ph.D. dissertation, University of Tennessee, Knoxville, 1982.
21. J. F. Rudd and E. F. Gurnee, *J. Appl. Phys.*, **28,** 1096 (1957).
22. V. M. Tsvetkov and E. A. Krym, *Vestnik Leningrad Univ., Ser. Mat. Fiz. Khim*, **3,** 5 (1956).
23. J. F. Rudd and E. F. Gurnee, *J. Polym. Sci., Polym. Chem., Ed.*, **1,** 2857 (1963).
24. M. F. Milagin, A. D. Gabarayeva, and I. I. Shishkin, *Polym. Sci. USSR*, **12,** 577 (1970).
25. V. K. Schmieder and K. Wolf, *Koll. Z.*, **134,** 149 (1953).
26. L. E. Nielsen, R. A. Wall, and P. G. Richmond, *Soc. Plast. Eng. J.*, **11** (Sept.) 22 (1955).
27. R. A. Wall, J. A. Sauer, and A. E. Woodward, *J. Polym. Sci.*, **35,** 281 (1959).
28. S. Newman and W. P. Cox, *J. Polym. Sci.*, **46,** 29 (1960).
29. A. V. Tobolsky and M. Takahashi, *J. Appl. Polym. Sci.*, **7,** 1341 (1963).
30. M. Takahashi, M. C. Shen, R. B. Taylor, and A. V. Tobolsky, *J. Appl. Polym. Sci.*, **8,** 1549 (1964).
31. F. R. Schwarzl, *Fifth International Rheological Congress*, Naples, 1980.
32. W. H. McAdams, *Heat Transmission*, 3rd ed., McGraw-Hill, New York, 1954.
33. R. Gardon, personal communication.
34. G. Goldbach and G. Rehage, *J. Polym. Sci., Symp. Ser.*, **16,** 2289 (1967).
35. A. J. Kovacs, *J. Polym. Sci.*, **30,** 131 (1958); *Rheol. Acta*, **5,** 262 (1966).
36. A. J. Kovacs, J. M. Hutchison, and J. J. Aklonis, in *The Structure of Non-Crystalline Materials*, P. H. Gaskell, Ed., Taylor and Francis, London, 1977.
37. L. C. E. Struik, *Physical Aging in Amorphous Polymers and Other Materials*, Elsevier, New York, 1978.
38. M. R. Tant and G. L. Wilkes, *Polym. Eng. Sci.*, **21,** 874 (1981).
39. K. C. Rusch, *J. Macromol. Sci., Phys.*, **132,** 179 (1968).
40. M. J. Richardson and N. G. Savill, *Polymer*, **18,** 3 (1977).
41. J. D. Ferry, *Viscoelastic Properties of Polymers*, 3rd ed., Wiley, New York, 1980.
42. B. D. Snow, M.S. thesis, University of Tennessee, Knoxville, 1982.
43. B. D. Aggarwala and E. Saibel, *Phys. Chem. Glasses*, **2,** 137 (1961).

Received October 1, 1982
Accepted January 14, 1983